Available at: http://www.ictp.it/~pub_off IC/2006/101

United Nations Educational, Scientific and Cultural Organization
and
International Atomic Energy Agency
THE ABDUS SALAM INTERNATIONAL CENTRE FOR THEORETICAL PHYSICS

GROWTH KINETICS OF METASTABLE (331) NANOFACET ON Au AND Pt(110) SURFACES

U.T. Ndongmouo, E. Houngninou
Institut des Mathématiques et des Sciences Physiques (IMSP)
et Département de Physique de l'Université d'Abomey-Calavi,
BP 613, Porto-Novo, Benin

and

F. Hontinfinde*
Institut des Mathématiques et des Sciences Physiques (IMSP)
et Département de Physique de l'Université d'Abomey-Calavi,
BP 613, Porto-Novo, Benin,
Dipartimento di Fisica dell'Universitá di Genova, Genova, Italy
and
The Abdus Salam International Centre for Theoretical Physics, Trieste, Italy.

Abstract

A theoretical epitaxial growth model with realistic barriers for surface diffusion is investigated by means of kinetic Monte Carlo simulations to study the growth modes of metastable (331) nanofacets on Au and Pt(110) surfaces. The results show that under experimental atomic fluxes, the (331) nanofacets grow by 2D nucleation at low temperature in the submonolayer regime. A metastable growth phase diagram that can be useful to experimentalists is presented and looks similar to the one found for the stationary growth of the bcc(001) surface in the kinetic 6-vertex model.

MIRAMARE – TRIESTE
December 2006

* Senior Associate of ICTP. Corresponding author: fhontinfinde@yahoo.fr

I. INTRODUCTION

Metastable states are commonly observed in nature and some of them can be extremely long-lived[1]. They can be found in various areas in physics: supercooled fluids[2], crystal surface growth[3], ferroelectrics[4], vortex states in superconductors[5], etc. The decay kinetics of these phases has been a subject of intense investigation in a wide variety of basic and applied contexts for several decades (see review in ref. [1]).

In this paper, we study the growth and decay of metastable (331) nanofacets on Au and Pt (110) surfaces. These surfaces usually reconstruct and show a two-dimensional (1x2) periodicity[6, 7]. It was established that they stabilize through (111) facets which represent their equilibrium phase. In epitaxial growth conditions, however, metastable (331) facets may appear due to some lack of surface relaxation between consecutive atom depositions[8, 9]. Their thermal growth and irreversible decay in the submonolayer regime is a complex problem of metastability that we qualitatively address in this work.

An epitaxial growth model of Au and Pt (110) surfaces is considered[8–10]. It comprises atom deposition and surface diffusion processes. The diffusion barriers used have been calculated by quenched Molecular Dynamics (MD) simulations with the many-body potentials developed by Rosato, Guillopé and Legrand (RGL) at the second neighbour cutoff[11]. These potentials favour the (1x2) reconstruction of the surfaces. Beyond single atomic motions, dimer and atomic chain mobility in the missing-rows (MRs) is considered, induced by the so-called leapfrog diffusion which has been experimentally[12] and theoretically[13] observed on these surfaces. It was recently shown by means of extensive numerical simulations that the latter drives the (111) facet stability[9]. From Ref. [9], the metastable (331) facet that appears during growth, decays with some average lifetimes that can be measured in some fractions of milliseconds to hours depending on the decay temperature. This perhaps explains why a (331) facet has rarely been observed on the Au(110) surface, even in Scanning Tunneling Microscopy (STM) studies around room temperature, unless the surface is strongly pinned by some defects[14]. The time decay mode at fixed temperature was clearly non-classical (non-exponential) and this suggested some periodicity in the spatial distribution of these facets on the surface[9]. The dynamics through which the decay occurs was suspected to be driven by the same leapfrog diffusion at the onset of atom detachment from chain islands. In the calculations, the (331) step density (referred to as the facet growth rate in the following) is evaluated. With increasing temperature T at fixed surface coverage θ and atomic flux f, this rate shows a maximum at a giving temperature before decreasing[8, 9]. This temperature referred to as T_{2sf} in Ref. [8] is taken as a transition temperature between the growth and decay modes of the metastable (331) phase. Considering several coverages, we construct a phase diagram that can be useful to experimentalists in overlayers deposition and catalysis. The phase diagram is similar to the one found previously for the growth modes of a bcc (001) surface in a kinetic 6-vertex model with only deposition and desorption kinetics[3, 15]. This analogy suggests that the metastable (331) facet growth should follow the 2D-classical nucleation theory (birth, growth and coaelscence of some critical 2D-nuclei)[15, 16].

The remainder of this work is organized as follows. In Section II, a brief insight is given on the kinetic 6-vertex model. Section III describes the growth model of the metastable (331) facet. In

sections IV and V, we present and discuss our results on the metastable growth phase diagram. Section VI is devoted to a concluding summary.

II. A BRIEF INSIGHT ON THE KINETIC 6-VERTEX MODEL

This is a temperature-model which describes the bcc(001) surface growth[3, 15]. The surface is mapped onto the 6-vertex model[17] according to van Beijeren[18]. Growth occurs in the model by atom deposition and evaporation following a generalized Glauber kinetics[19]. The deposition rate is given by:

$$C^a = \frac{exp(\Delta\mu/kT)}{1 + exp(\Delta E^a/kT)} \tag{1}$$

and the desorption rate by:

$$E^a = \frac{1}{1 + exp(\Delta E^a/kT)} \tag{2}$$

where $\Delta\mu$ is the driving force, T the absolute temperature, ΔE the surface energy change (due to the process) expressed in units of ϵ which is the 6-vertex energy and the superscript 'a' is related to the coordination number of the growth or evaporation site. The kinetic equation of this model can be solved exactly on small system sizes by the transition matrix method after the classification of surface 6-vertex configurations into time-conserved classes and non-conserved subclasses[3, 15]. Kinetic Monte Carlo simulations are used for large systems[3, 15]. The exact calculation yields the subclasses' weights used to evaluate the exact growth rate G of the bcc(001) surface. For more details, the reader should refer to references [3, 15, 20]. This toy model is completely different from the complicated but physical one given below (in section III) for the (331) nanofacet growth, where the surface relaxation occurs by some anisotropic surface diffusion due to the (110) surface topography. However, both models show some similar trends that may help in getting some insight into the growth mechanism of (331) metastable facet on Au and Pt (110) surfaces, at least at low temperature.

Let us consider a 4x6 bcc(001) surface. The kinetic growth equation of this sample involves a 1384x1384 transition matrix. Exact results on the growth rate from our calculations are given in Fig.1a for fixed values of the reduced driving force $\Delta\mu/T_R$ and varying reduced temperature T/T_R. The temperature $T_R = \epsilon/Log(2)$ is the equilibrium roughening transition temperature of the surface[18]. The curves show an exponential increasing part. This behaviour of the growth rate has been used in Ref. [15] to build a growth phase diagram for the bcc(001) surface, relying on the temperature associated to the maximun growth rate. Using this approach for the 4x6 system, one gets the growth phase diagram displayed in Fig.1b. At low temperature and small disequilibria, the growth occurs in a layer-by-layer mode. There, the growth rate follows the Becker-Doering law [3, 15, 16]:

$$G \simeq (\Delta\mu/kT)\exp(-E_s^2/3kT\Delta\mu), \tag{3}$$

where E_s is proportional to the step free-energy per unit length. At high temperature or very high driving force, the growth occurs continuously and particles can fall everywhere on the surface

forming hillocks. In the following, we use the same approach to construct a metastable growth phase diagram for the (331) nanofacet on Au and Pt(110) surfaces. There is some evidence for layer-by-layer growth in the kinetic 6-vertex model. However, the stationary growth aspect of a non-equilibrium crystal surface is that of a rough surface. Layer-by-layer crystal growth in real systems could either occur in the early stage of the growth or be due to finite-size effects.

III. MODEL OF (331) NANOFACET GROWTH

In most crystal growth processes of current interest, surface diffusion plays an important role. In this model, the desorption is neglected and the surface fully relaxes through surface diffusion (see Refs. [8–10]).

Atoms are randomly deposited on the surface at a constant flux f. Cascades and downward funneling of the deposited atom are considered. The diffusion processes are depicted in Fig.2 and their energy barriers in Table 1 (taken from Ref. [9]) have been calculated with the RGL potentials developed on the basis of the second moment approximation to the tight-binding model[11]. The diffusion rate has the Arrhenius form $\nu \exp(-E/kT)$ where E is the diffusion barrier and the prefactor ν set to $10^{12} s^{-1}$ for all diffusive motions. E comprises the diffusion barrier on the bare substrate which costs E_p^0 (process p_1) in the [$1\overline{1}$ 0] direction and E_n^0 (process p_3) in the [001] direction, and also depends on the number n_p of strong in-channel bonds of energy E_p^b and n_n of weak cross-channel bonds of energy E_n^b of the diffusing atom as follows[8–10]:

$$E_p \;=\; E_p^0 \;+\; n_p E_p^b \;+\; n_n E_n^b; \tag{4}$$

$$E_n \;=\; E_n^0 \;+\; n_p E_p^b \;+\; n_n E_n^b. \tag{5}$$

Thus, from Fig.2 and Table I, process p_7 costs 0.96 eV and process p_8 costs 0.63 eV on the Pt(110) surface. In the cross-channel ([001]) direction, diffusion essentially occurs by exchange (process p_3), because the direct jump is too costly (process p_4). Step-descent (process p_5) and the leapfrog diffusion (process p_6) energy barriers are respectively denoted by E_p^S and E_{lf}.

The model is solved using the Monte Carlo algorithm developed by Bortz, Kalos and Lebowitz [21] which is a coarse-grained lattice-based atomistic technique [8–10]. All possible processes occuring during the growth are assumed to be statistically independent. From their rates $k_i, i = 1, p$, where p is the number of processes recorded at a given step of the simulations, the total evolution rate $K = \sum_{i=1}^{p} k_i$ by deposition and diffusion is calculated and mapped onto the unit interval by normalizing all rates k_i by K. A random number is drawn to select either a deposition or a diffusion process. Then one specific transition of the list is randomly selected and realized with probability 1. The real growth time increment Δt which follows Poisson statistics depends also on K and is given by : $\Delta t = -Log(r)/K$ where r is a generated random number, $0 < r < 1$ (see [8–10] and references therein for more details).

The (331) metastable step of unit length (see Fig.3) in the [$1\overline{1}$ 0] direction is described on the growing surface by the Ising-type subconfiguration (+1,+1,-1,+1,+1) in the [001] direction, (+1) for a step-up and (-1) for a step-down, starting from both sides of the (110) growing surface. The

(331) step density (referred to as the growth rate) is just the total number of such subconfigurations found on the surface normalized by the surface area or by the total number of surface sites.

IV. GROWTH MODES OF THE (331) NANOFACET

The initial substrate configuration considered in the following is a (1×2) reconstructed Au(110) or Pt(110) surface of size 128×64 and/or 128×128 with periodic boundary conditions in both [1 $\overline{1}$0] and [001] directions. The [1 $\overline{1}$0] direction is that of the atomic rows. The deposition flux is first kept constant, and set to the experimental value: $f = 0.0167$ monolayer per second (ML/s). For small surface coverages, 20 independent runs are performed whereas for larger coverages ($\theta > 0.5$), 30 independent runs are made for a meaningful statistical average of the (331) step density which is indeed, proportional to the (331) facet growth rate.

Figure 4 gives the (331) facet growth rate at fixed deposition flux for several values of θ. The growth rate G shows an increasing part, a maximum and then decreases with increasing temperature T. Let us mention that the (331) nanofacet growth rate is completely different from the growth rate of the whole surface which is a constant at all temperatures. The temperature associated to the maximum rate (denoted by T_{2sf} in Ref. [8]) decreases with increasing surface coverage. This feature of the growth rate looks similar to the one found previously (in Fig.1) in the Kinetic 6-vertex model for the bcc(001) surface growth[3, 15]. The exponential increasing part of the growth rate G should suggest that the nanofacet grows in this region by some 2D-nucleation on the Au(110) and Pt(110) surfaces.

In the kinetic 6-vertex model, the deposition rate depends on the supersaturation $\Delta\mu/kT$[3, 15]. Let us assume that the atomic flux f behaves as $\exp(\Delta\mu/kT)$ or simply that $f \sim \Delta\mu/kT$ for very small supersaturation. Thus, $G \sim f \exp(-E_s^2/3(kT)^2 f)$, with E_s denoting the step bordering the (331) facet free-energy. The quantity E_s does exist if one can find a temperature domain where the curve $fLog(G/f)$ as a function of $1/(kT)^2$ shows a linear part. In Fig.5, this function is displayed. The linearity exists at low temperature for both (110) surfaces. We then speculate that there is an evidence for a layer-by-layer facet growth that can be decribed by the classical 2D-nucleation theory[17]. Some critical (331) nanofacet nuclei are then formed in the initial stage of the facet growth. Then they spread on the surface by preferentially receiving diffusing atoms in the in-channel direction. This is in fact, an interesting example of growth by 2D-nucleation in the presence of surface diffusion. Surface diffusion has in general a destabilizing effect and leads to unstable growth[20]. The advent of surface instability during growth induced by step-edge barriers and the corresponding uphill mass current[20, 22] can then generate specific phases on crystal surfaces that are different from the equilibrium one (as in the present case).

A schematic phase diagram is constructed following the same scenario used above in the case of the bcc(001) surface. We then look for the temperature of the maximum growth rate at each coverage. The corresponding metastable diagram is displayed in Fig.6a,b for both (110) surfaces. From Fig.6a, it emerges that there are some finite-size effects on the results for the 128x64 system. With increasing system size, the volume of the layer-by-layer domain slowly decreases; we however suspect that this mode may persist in the thermodynamic limit at least at low temperature and

relatively large coverage or at very small coverages and high temperature. Such decrease of the 2D-nucleation domain has been also observed in the kinetic 6-vertex model[3]. Well below the transition lines in Fig.6a,b, layer growth of the (331) facet is expected. Above, an irreversible dynamical conversion of the (331) nanofacet to the more stable (111) one occurs[9]. We check that this decay of the metastable phase driven by the leapfrog mobility is almost associated to the onset of atom detachment from chain islands. Thus the decay is thermally activated and an exponential decrease with the temperature is expected. The behaviour of the facet growth rate at high temperature (after T_{2sf}) in Fig.4b supports this finding at least for very small coverages. The region of irreversible facet decay can be viewed as a continuous facet growth domain. Indeed, the particles landing on islands and the leapfrogging ones can make sparse chain islands on the surface, that increase the (111) step density (and also the interface width) but destroy locally the compactness of the growing (331) facet. The surface may then be covered by sparse (331) nanofacets as happens to surface islands in the early stage of a continuous growth.

Contrarily to the previous results, the temperature T_{2sf} increases with increasing deposition flux f. This can be understood as follows. From reference [8], the onset temperature where (331) and (111) facet densities start to increase in equal proportions, denoted by T_{1sf} and referred to as the first selective faceting temperature, depends on the model parameters as:

$$T_{1sf} \simeq (2E_{up} - E_{down})(kLog(\frac{2m\theta\nu}{f}))^{-1} \tag{6}$$

where $E_{up} = 0.84\ eV$, $E_{down} = 0.64\ eV$ for Pt(110), ν is the prefactor of the diffusion rates and m the average chain island length. T_{1sf} increases with f, then the whole growth rate curve is shifted to higher temperatures. This explains why T_{2sf} increases with f. We then find convenient to draw the phase diagram in the $(1/(kT), f)$ plane as in Fig.6c. Below the transition line the (331) facet decays, whereas above it grows by the 2D-nucleation mechanism. One can realize that the decrease of T_{1sf} as a function of θ observed in the previous formula also induces a decrease of T_{2sf} as found in Fig.4.

It is important to stress that the facet does not grow in a layer-by-layer mode in the whole layer growth regions mentioned in Fig.6. From Fig.7, there is some evidence that the (331) nanofacet does not grow once the atomic flux is set on the surface. There exist a time interval where the surface fluctuations do not produce any (331) facet. This clearly suggests the existence of a barrier (free-energy) cost (known as the Gibbs' measure of surface stability) to build a critical (331) facet. This result supports the 2D-nucleation mechanism found above. This 'Gibbs' domain of stability' of the (110) surfaces against the production of metastable (331) facets depends on the temperature. We measure its width with respect to the real time associated to the last random walk to zero of the number of nucleated (331) nanofacets during the surface fluctuations. We find from Fig.7a, 0.83 s at $T = 470\ K$; 1.10 s at $T = 440\ K$; 1.19 s at $T = 430\ K$ and 1.45 s at $T = 420\ K$. Gibb's domain decreases with the increasing temperature. This is not surprising because the up-promotion by leapfrog is thermally activated in the model.

We also study how the total number N of nucleated (331) nanofacets evolves with the growth time at fixed $f = 1\ ML/mn$ and T in the submonolayer growth regime. A tendency to some oscillatory behaviour exists. In the early stage of the growth, N evolves as a power-law of the growth

time (see Fig.7b): $N \sim t^{\beta}$ where β is a temperature-dependent time exponent. At $T = 430\ K$, $\beta \simeq 2.69$ whereas at $T = 470\ K$, $\beta \simeq 3.35$ for a Pt(110) surface of size $L = 128$.

Another fcc(110) surface that shows similar trends is the Ir(110) surface. There, the stabilization occurs through (331) facets while (111) facets are metastable[9]. A metastable (111) phase diagram for the Ir(110) surface could also be constructed as in Fig.6.

One open question is whether the 2D-nucleation mechanism observed still prevails in the stationary growth stage of the surface. This is hard to check within the present model due to the large computation time needed. In the following a 1D-version of the growth model[23] is exactly solved on a finite sample to give some ideas on such problem.

V. A 1D MODEL FOR (331) FACET GROWTH

The model is defined on the single step of length $L = 16$ of Fig.3 which may be viewed as a single atomic chain formed by the surface atoms of a two-dimensional crystal growing from an atomic beam. The single step is assumed now to be oriented in the $[1\overline{1}0]$ direction. The growth occurs through atom deposition and diffusion. The diffusion processes are: in-channel diffusion, step-descent by jump, upward atom promotion by leapfrog, dimer rigid motion, atom detachment from chain islands. Only the cross-channel diffusion by exchange is missing in the dynamics. The relation (4) becomes: $E = E_p^0 + n_p E_p^b$ where where n_p can be 0 or 1. The model is exactly solved for $L = 16$ by the transition matrix method and a 810x810 matrix is involved. Let P_m^{∞} denote the normalized mth subclass weight in the steady state, N_m^{331} the number of (331) step in the mth subclass, the exact steady state (331) step density (growth rate) is given by:

$$\overline{N} = \sum_m P_m^{\infty} N_m^{331}. \tag{7}$$

The results are displayed in Fig.8 for both Au and Pt (110) surfaces as a function of the temperature for $f = 1\ ML/mn$. The system seems somewhat chaotic in the steady state with some fluctuations in the numerical results. It emerges that an exponential increasing part and a maximum exist on the curves. One gets $T_{2sf} = 210\ K$ for Au(110) and $T_{2sf} = 405\ K$ for Pt(110) surface. Although a small sytem is used in the investigation the results seem to be consistent with the phase diagrams in Fig.6a,b. A (331) facet growth by 2D-nucleation is then suspected in the steady state on Au and Pt(110) surfaces.

VI. CONCLUSIONS

In this work we study, by kinetic Monte Carlo simulations, a realistic growth model with surface diffusion to single out the growth mechanisms of metastable (331) nanofacets on Au and Pt(110) surfaces in the submonolayer regime. The growth rate at the onset of the upward leapfrog atomic diffusion increases with temperature at fixed coverage and presents a maximum at a certain temperature that is taken as a transition temperature between two growth modes of the facet: 2D-nucleation mechanism and the irreversible activated decay. Such approach was used in the kinetic

6-vertex model for the bcc(110) surface growth that we briefly described. This feature enabled us to construct a metastable growth phase diagram for both surfaces. We also isolated in the layer-by-layer domain a region in the model parameters' space where the (110) surfaces resist against the metastable (331) facet growth. There, the surface is in metastable equilibrium (although $f \neq 0$) with the fluid phase with respect to the growth of (331) facet as it often happens in supercooled or supersaturated fluids. Our calculations also indicate that the total number of nucleated (331) nanofacets evolves as a temperature-dependent power-law with the whole surface growth time in the early stage of the facet growth. Finally, a one-dimensional version of the (331) facet growth model is exactly investigated (on a small sample) to show that the 2D-nucleation mechanism still prevails at very high coverage.

Acknowledgments

The authors thank Profs. A. Levi, R. Ferrando and R. Rousseau for a critical reading of the manuscript. This work was done within the framework of the Abdus Salam International Centre for Theoretical Physics, Trieste, Italy, where most of the calculations reported in this work have been performed. Financial support from the Swedish International Development Cooperation Agency (SIDA) is acknowledged.

References

[1] P. A. Rikvold and B. M. Gorman, Cond-mat/9407027, July 1994.

[2] F. F. Abraham, Homogeneous Nucleation Theory (Academic, New-York, 1974).

[3] F. Hontinfinde and M. Touzani, Surf. Sci. **338**, 236 (1995).

[4] Y. Ishibashi and Y. Takagi, J. Phys. Soc. Jpn **31**, 506 (1971); P. Chandra, Phys. Rev. A **39**, 506 (1971).

[5] Y, N, Ovchinnikov and I. M. Sigal, Phys. Rev. B **48**, 1085 (1993).

[6] S. Speller, F. Kuntze, T. Rauch, B. Bomermann, M. Huck, M. Aschoff and W. Heiland, Surf. Sci. **366**, 251 (1996).

[7] G. Binnig, H. Rohrer, Ch. Gerber and E. Weibel, Surf. Sci. **131**, L379 (1983).

[8] F. Hontinfinde, A. Videcoq, F. Montalenti and R. Ferrando, Chem. Phys. Lett. **398**, 50 (2004).

[9] U. T. Ndongmouo, F. Hontinfinde and R. Ferrando, Phys. Rev. B **72**, 115412 (2005).

[10] A. Videcoq, F. Hontinfinde and R. Ferrando, Surf. Sci. **515**, 575 (2002).

[11] F. Rosato, M. Guillopé and B. Legrand, Philos. Mag. A **59**, 321 (1989); F. Ducastelle, J. Phys. (Paris) **31**, 1055 (1970).

[12] T. R. Linderoth, S. Horch, L. Petersen, S. Helveg, E. Laegsgaard, I. Stensgaard and F. Besembacher, Phys. Rev. Lett. **82**, 1484 (1999).

[13] F. Montalenti and R. Ferrando, Phys. Rev. Lett. **82**, 1498 (1999).

[14] M. J. Rost, R. van Gastel and J. W. M. Frenken, Phys. Rev. Lett. **84**, 1966 (2000) and references therein.

[15] M. Kotrla and A. C. Levi, J. Stat. Phys. **64**, 579 (1991).

[16] R. Becker and W. Doering, Ann. Phys. (Leipzig) **24**, 179 (1935).

[17] R. J. Baxter, Exactly Solvable Models in Statistical Physics, Academic Press, London, 1982.

[18] H. van Beijeren, Phys. Rev. Lett. **38**, 993 (1977).

[19] R. J. Glauber, J. Math. Phys. **4**, 294 (1963).

[20] F. Hontinfinde, J. Krug and M. Touzani, Physica A **237**, 363 (1977).

[21] A. B. Bortz, M. H. Kalos and J. L. Lebowitz, J. Comput. Phys. **17**(1), 10 (1975)

[22] J. Krug and F. Hontinfinde, J. Physics A: Math. Gen. **30**, 7739 (1997).

[23] F. Hontinfinde, R. Ferrando and A. C. Levi, Physica A **319**, 36 (2003).

TABLE I: Energy barriers for some diffusion processes (see Fig.2 for description) and bond energies (in eV) considered in the missing-row (110) surface growth model.

Energy	Au(110)	Pt(110)
$E_p^0(p_{1,2})$	0.33	0.60
$E_n^0(p_3)$	0.46	0.80
$E_p^S(p5)$	0.37	0.64
$E_{lf}(p_6)$	0.45	0.84
E_p^b	0.21	0.36
E_n^b	0.01	0.03

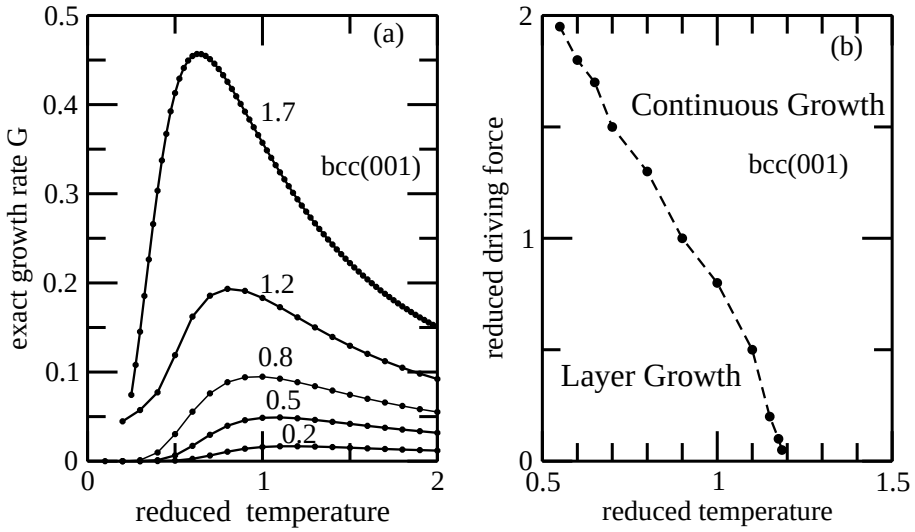

FIG. 1: Exact growth rate in the kinetic 6-vertex model (panel a) for a non-sloped 4x6 bcc(001) surface at fixed values of the reduced driving force $\Delta\mu/T_R$ (as labeled on the curves) and varying reduced temperature T; panel b gives the corresponding growth phase diagram as described in the text. Kinetic Monte Carlo simulations from Ref.[3] on larger sizes have shown that the layer growth domain slowly decreases with increasing system size.

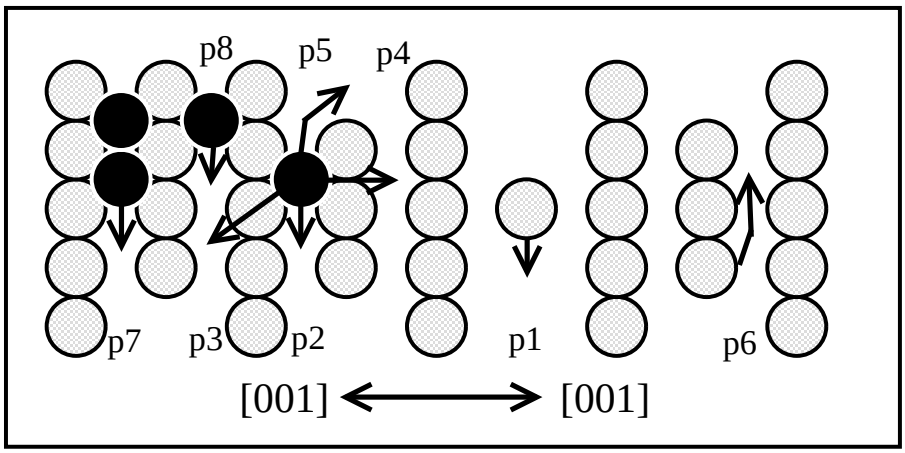

FIG. 2: Atom diffusion processes on Au and Pt(110) surfaces. Grey atoms are at level 0. Black atoms are at level 1. Process p_1: single atom diffusion in a missing-row; process p_2: in-channel diffusion on a (1x1) facet of the surface. Process p_3 is a cross-channel diffusion by an exchange mechanism; process p_4: direct cross-channel jump (too costly and not considered in the simulations); process p_5: step-descent in the in-channel direction; process p_6: leapfrog upward promotion of an atom at the end of an atomic chain in the missing-row. Process p_7 is an in-channel move that breaks one in-channel bond whereas process p_8 is an in-channel diffusion that breaks a cross-channel bond. The [001] direction is indicated by a double-head arrow in the figure.

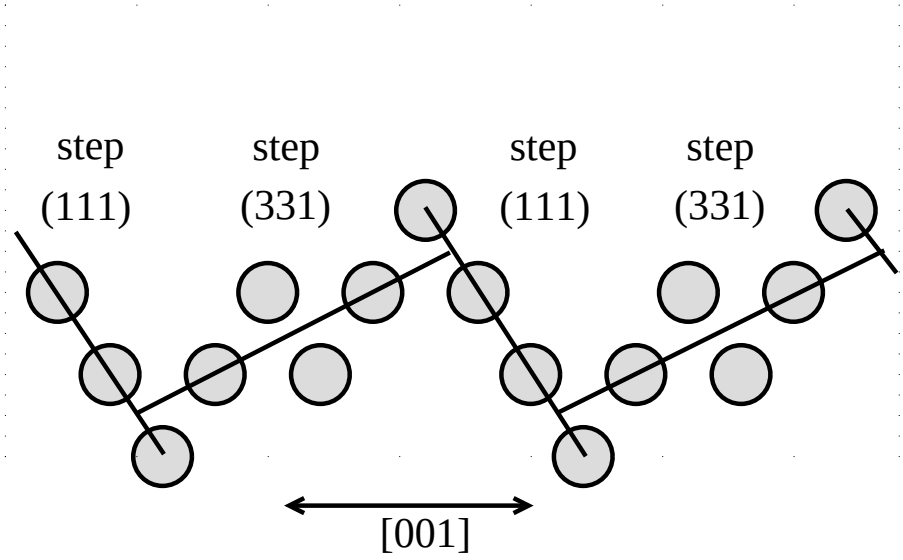

FIG. 3: A schematic representation in the [001] direction of a metastable (331) step and a more stable (111) step of unit length in the $[1\overline{1}0]$ direction. The atomic chain with length $L = 16$ of the figure, can be viewed as formed by the surface atoms of a two-dimensional crystal growing from an atomic beam.

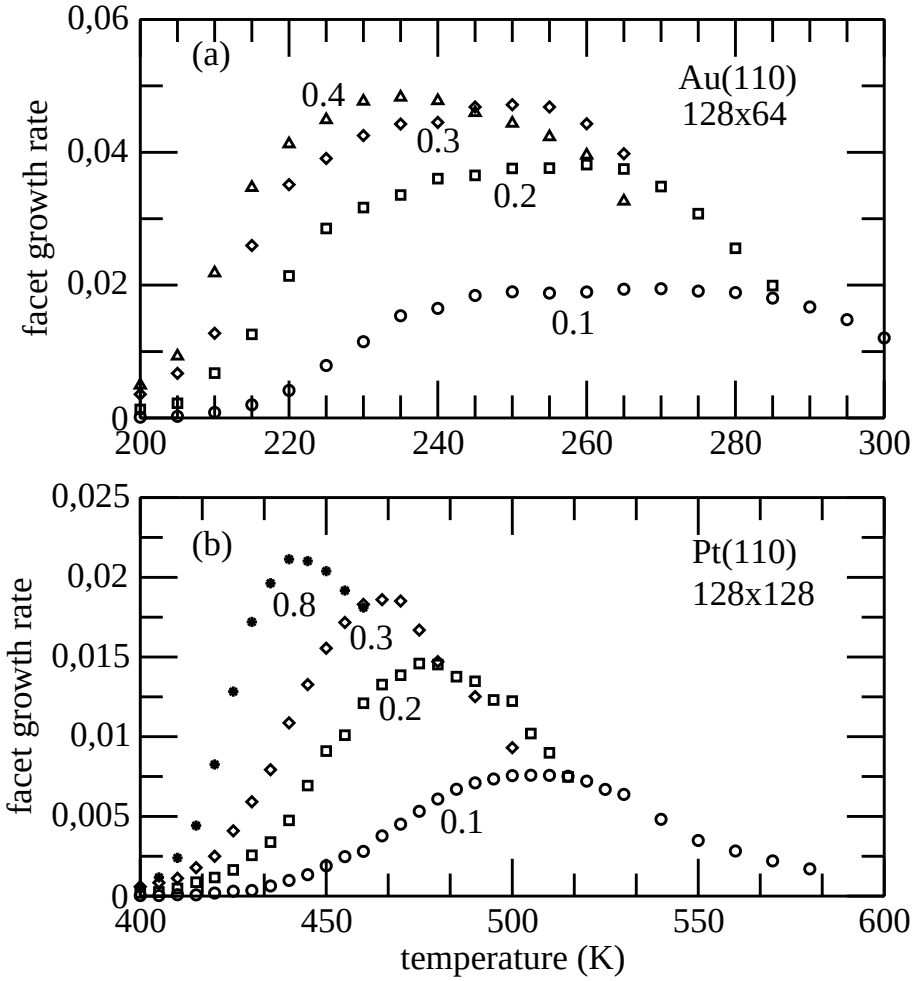

FIG. 4: The metastable (331) nanofacet simulated growth rate as a function of the temperature for Au(110) (panel a) and Pt(110) (panel b) at fixed values of the coverage (as labeled on the curves) and constant deposition flux $f = 1$ ML/mn. For Au(110), a 128x64 system is used whereas for Pt(110), a 128x128 system is considred.

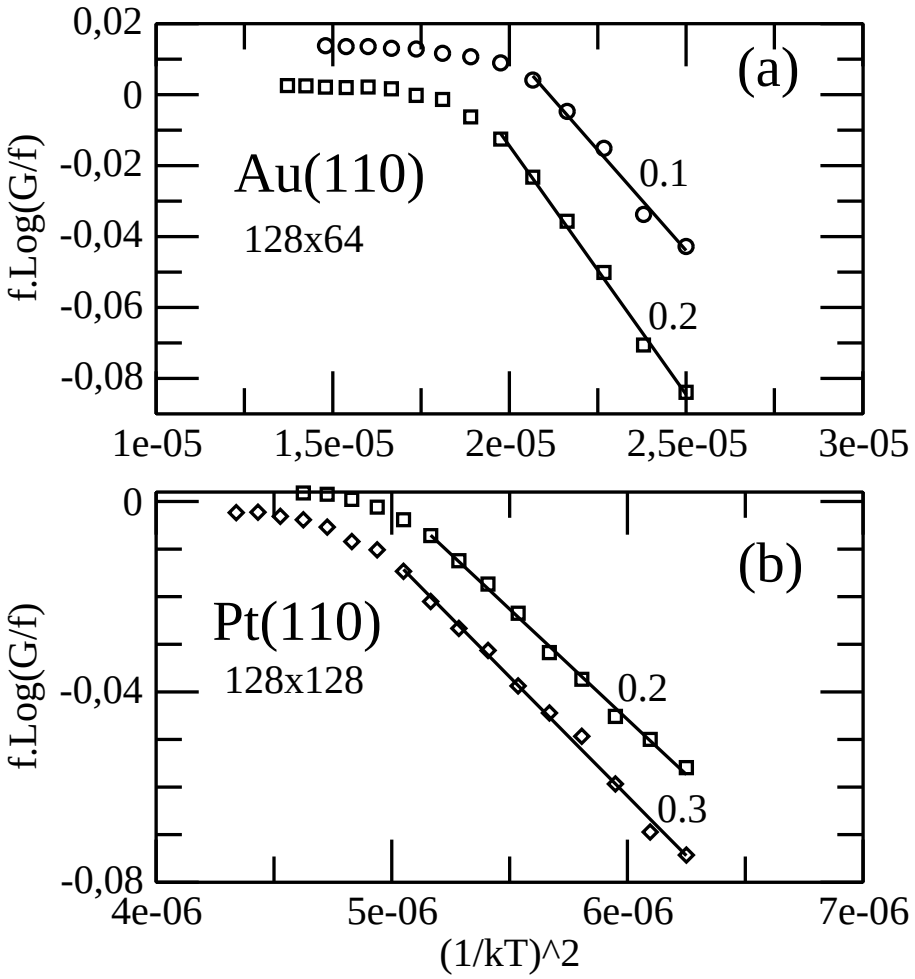

FIG. 5: The functions $f.Log(G/f)$ *vs* $(1/kT)^2$ at two fixed values of the surface coverage (as labeled on the curves) and $f = 1$ ML/mn for Au (panel a) and Pt(110) (panel b) surfaces. The existence of a temperature domain where the curves are linear indicates that the (331) facet grows in this region by some 2D-nucleation on both surfaces.

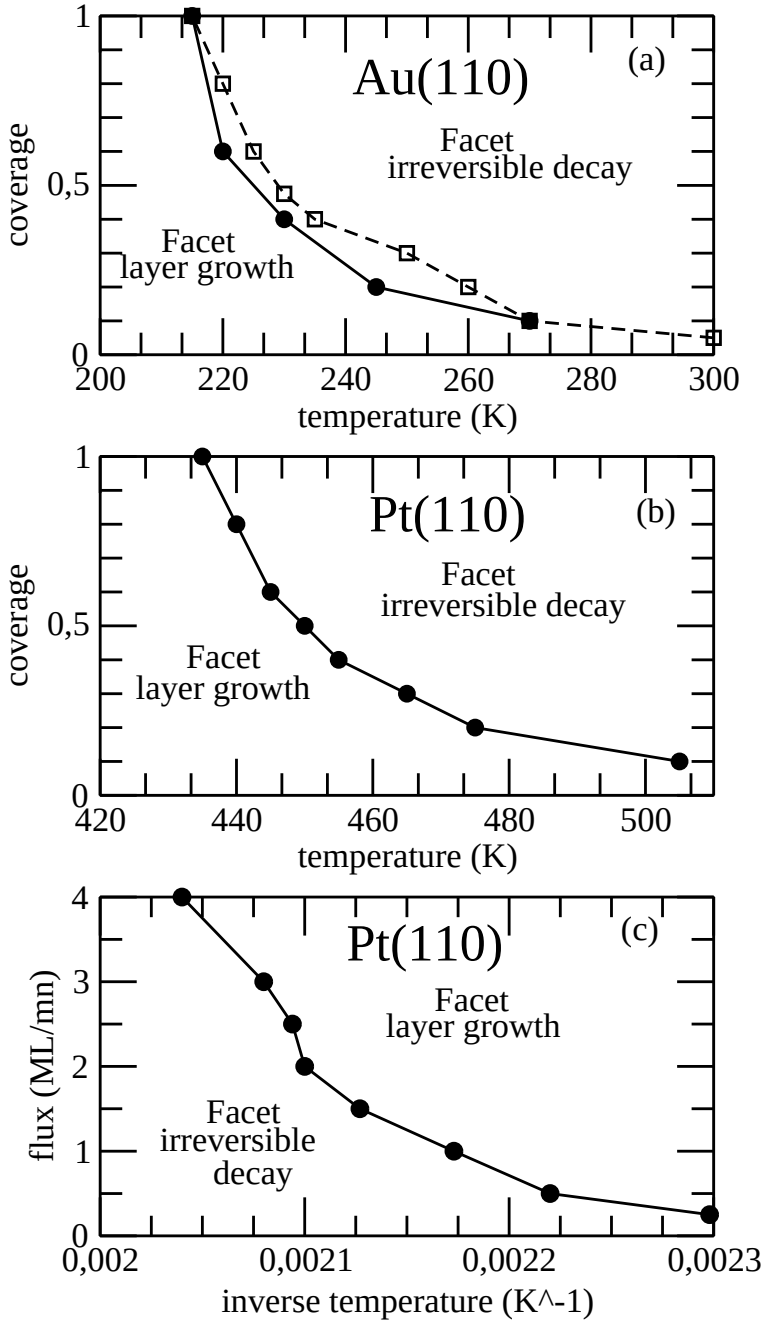

FIG. 6: Metastable (331) nanofacet growth phase diagrams for Au(110) (panel *a*) and Pt(110) (panel *b*) surfaces. In all panels, lines are those limiting the two growth modes of the nanofacet, the circles referring to a 128x128 system and the squares to a 128x64 system. Finite-size effects appear very weak at high temperature and small coverages and also at low temperature and relatively large coverages (see panel *a*). In panel c, the phase diagram is given in the (1/kT, f) plane for $\theta = 0.3$ and Pt(110) surface.

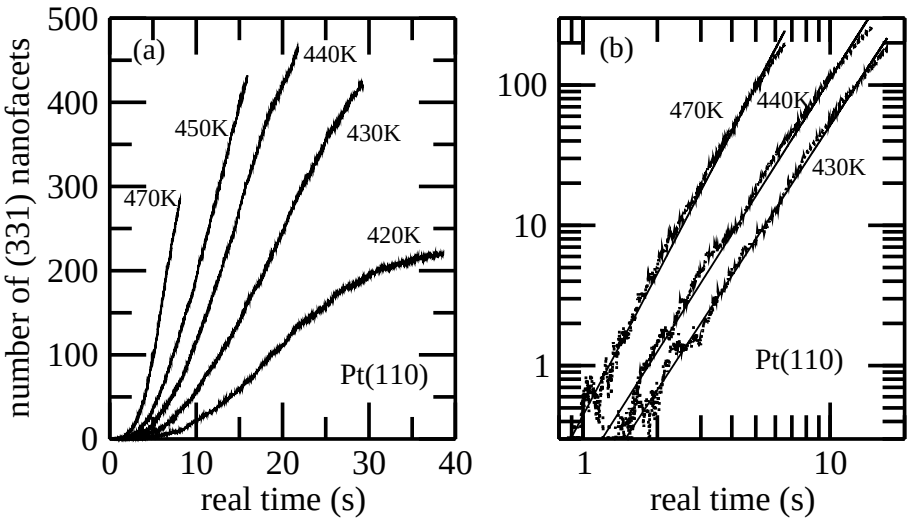

FIG. 7: Panel a: time evolution of the number N of nucleated (331) nanofacets at different temperatures for a 128x128 surface of Pt(110). In Panel b, log-log plots of N at three temperatures are presented and appear linear. This suggests the existence of a power-law behaviour of N with the real growth time. The numerical results displayed have been averaged over 30 independent runs.

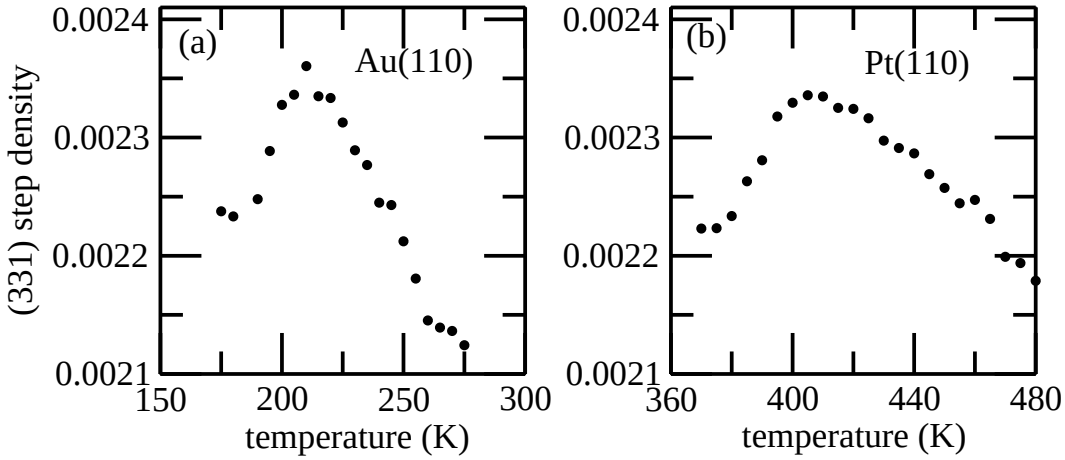

FIG. 8: Exact steady state (331) facet growth rate in the 1D-version of the growth model for Au and Pt(110) surfaces (see text). The curves show an exponential increasing part and a maximum at very large coverage.